

# The Effect of the DNA Conformation on the Rate of NtrC activated Transcription of *Escherichia coli* RNA Polymerase · $\sigma^{54}$ Holoenzyme

Alexandra Schulz, Jörg Langowski and Karsten Rippe\*

Deutsches  
Krebsforschungszentrum,  
Abteilung Biophysik der  
Makromoleküle, Im  
Neuenheimer Feld 280  
D-69120, Heidelberg  
Germany

The transcription activator protein NtrC (nitrogen regulatory protein C) can catalyze the transition of *Escherichia coli* RNA polymerase complexed with the sigma 54 factor (RNAP ·  $\sigma^{54}$ ) from the closed complex (RNAP ·  $\sigma^{54}$  bound at the promoter) to the open complex (melting of the promoter DNA). This process involves phosphorylation of NtrC (NtrC-P), assembly of an octameric NtrC-P complex at the enhancer sequence, interaction of this complex with promoter-bound RNAP ·  $\sigma^{54}$  via DNA looping, and hydrolysis of ATP. We have used this system to study the influence of the DNA conformation on the transcription activation rate in single-round transcription experiments with superhelical plasmids as well as linearized templates. Most of the templates had an intrinsically curved DNA sequence between the enhancer and the promoter and differed with respect to the location of the curvature and the distance between the two DNA sites. The following results were obtained: (i) a ten- to 60-fold higher activation rate was observed with the superhelical templates as compared to the linearized conformation; (ii) the presence of an intrinsically curved DNA sequence increased the activation rate of linear templates about five times; (iii) no systematic effect for the presence and/or location of the inserted curved sequence was observed for the superhelical templates. However, the transcription activation rate varied up to a factor of 10 between some of the constructs. (iv) Differences in the distance between enhancer and promoter had little effect for the superhelical templates studied.

The results were compared with theoretical calculations for the dependence of the contact probability between enhancer and promoter expressed as the molar local concentration  $j_M$ . A correlation of  $j_M$  with the transcription activation rate was observed for values of  $10^{-8} \text{ M} < j_M < 10^{-6} \text{ M}$  and a kinetic model for NtrC-P-catalyzed open complex formation was developed.

© 2000 Academic Press

**Keywords:** transcription initiation; enhancer; DNA looping;  
DNA curvature; local concentration

\*Corresponding author

## Introduction

Long-range interactions in DNA play an important role in the regulation of transcription: the distance on the DNA between regulatory sequences (enhancers) that constitute binding sites for gene-specific protein factors and the transcription

machinery at the promoter is often several hundreds or thousands of base-pairs. Contact between proteins at the enhancer and the promoter can be mediated by looping of the intervening DNA. This regulation mechanism appears to be of general importance in eukaryotes (Blackwood & Kadonaga, 1998; Dunaway & Dröge, 1989; Müller *et al.*, 1989; Ptashne & Gann, 1997). It is found also in a number of prokaryotic genes (Gralla & Collado-Vides, 1996; Reitzer *et al.*, 1989; Rippe *et al.*, 1997; Su *et al.*, 1990; Wedel *et al.*, 1990). In *Escherichia coli* these promoters are characterized by a special consensus sequence that requires the RNA

Abbreviations used: RNAP ·  $\sigma^{54}$ , RNA polymerase ·  $\sigma^{54}$  holoenzyme; RNAP ·  $\sigma^{70}$ , RNA polymerase ·  $\sigma^{70}$  holoenzyme; NtrC, nitrogen regulatory protein C.

E-mail address of the corresponding author:  
Karsten.Rippe@dkfz-heidelberg.de

polymerase complexed with the  $\sigma^{54}$  factor (RNAP· $\sigma^{54}$ ).

For transcription initiation, RNAP· $\sigma^{54}$  at the promoter has to interact with an activator protein like NtrC (nitrogen regulatory protein C, also designated as NR<sub>i</sub>) bound at the enhancer sequence *via* looping of the intervening DNA. For the experiments described here we have used a minimal system to study transcription activation by enhancer that consists of a DNA template with the *glnAp2* promoter, the enhancer sequence with two strong NtrC binding sites, RNAP· $\sigma^{54}$  holoenzyme and the NtrC activator protein. Upon hydrolysis of ATP, the phosphorylated form of NtrC (NtrC-P) catalyzes the transition of RNAP· $\sigma^{54}$  from the closed complex to the open complex. This is an important difference from the standard holoenzyme form of *E. coli* RNA polymerase (RNA polymerase· $\sigma^{70}$  holoenzyme, RNAP· $\sigma^{70}$ ), which can initiate open complex formation from a promoter without the interaction with an additional activator protein and/or hydrolysis of ATP. The *in vivo* upstream sequence of the *glnAp2* promoter contains two strong NtrC binding sites (−148 to −132 and −116 to −100 upstream of the transcription start site) and three weak NtrC sites (position −94 to −81, −73 to −60, and −53 to −37). The two strong sites are essential and sufficient for the activation reaction (Magasanik, 1996; Porter *et al.*, 1995; Reitzer & Magasanik, 1986; Reitzer *et al.*, 1989). They can be separated by 3000 base-pairs from the promoter, without a significant reduction of the transcription activity (Buck *et al.*, 1986; Reitzer & Magasanik, 1986; Wedel *et al.*, 1990).

The probability of an interaction between NtrC protein bound at the enhancer and RNAP· $\sigma^{54}$  at the promoter depends on the flexibility, length, and conformation of the intervening DNA. The contact probability can be expressed as the local concentration in moles per liter of the enhancer in the proximity of the promoter. This concentration in moles per liter will be called  $j_M$  in the following. One can think of  $j_M$  as the concentration of one protein that would be required free in solution (*in trans*) without a DNA linker to obtain the same contact probability. This is an old concept from polymer chemistry (Jacobson & Stockmayer, 1950). In DNA cyclization experiments the dependence of the local concentration on the DNA length has been studied (Crothers *et al.*, 1992; Hagerman & Ramadevi, 1990a,b; Shore & Baldwin, 1983; Shore *et al.*, 1981). In these experiments a distance of about 500 base-pairs between the two ends to be ligated was found to be optimal for the cyclization reaction. The apparent similarity of this reaction and protein-protein interactions mediated by DNA-looping has also been used to describe interactions between *lac* repressor proteins bound at separate DNA sites *in vivo* (Bellomy & Record, 1990; Mossing & Record, 1986). As compared to the cyclization experiments for the protein-protein interactions also factors like the size of the interact-

ing protein complexes and the occupancy of the respective binding sites have to be considered (Merlitz *et al.*, 1998; Rippe *et al.*, 1995). The expected interaction probabilities given in the latter two papers are in excellent agreement with the experimentally determined recombination frequency of the site-specific FLP recombinase for sites on linear substrates with a separation distance from 74 bp to 15 kb apart (Ringrose *et al.*, 1999).

For regular linear DNAs of a length from 100 to several thousand base-pairs a local concentration of the enhancers in the vicinity of the promoter of  $10^{-7}$  to  $10^{-9}$  M has been calculated (Merlitz *et al.*, 1998; Rippe *et al.*, 1995). Assuming a volume of  $1 \mu\text{m}^3$  for a single *E. coli* cell, the intracellular concentration of NtrC dimers has been determined to be around  $10^{-8}$  M in the inactive state (Reitzer & Magasanik, 1983). Under nitrogen limiting conditions the NtrC dimer concentration rises to  $10^{-7}$  M. Thus, for a linear DNA fragment DNA-looping would have little effect on the interaction probability of RNAP· $\sigma^{54}$  with a single NtrC dimer, since the local concentration  $j_M$  due to DNA-looping would be similar or even lower than the concentration at which NtrC is already present in solution. In this context it is important to note that binding of NtrC-P to the enhancer DNA sequence which contains two binding sites also induces the formation of a specific octameric NtrC-P complex (Rippe *et al.*, 1998). The concentration of this complex in the absence of the enhancer sequence is likely to be much lower than that of the NtrC dimer. Thus, the DNA linkage between enhancer and promoter can facilitate interactions that would not occur if the proteins were free in solution. This idea is consistent with the observation that eukaryotic enhancers often contain multiple protein binding sites that act synergistically (Carey, 1998) and is supported by the formation of  $\lambda$  repressor octamer by DNA-looping-mediated interactions of  $\lambda$  repressor tetramers (Révet *et al.*, 1999).

In addition, DNA is a flexible polymer and can adopt different conformations, some of which promote the interaction between distant sites. For example, *in vivo* DNA is superhelical, i.e. it adopts a higher-order structure due to torsional strain (reviewed by Bates & Maxwell (1993)). This conformation is found in the circular DNA of plasmids, bacterial chromosomes, chloroplasts, mitochondria, and viruses. Furthermore, linear chromosomal DNA of eukaryotes is organized by proteins in loops of 100 to 150 kb which form topological domains in which the DNA is also negatively supercoiled. It is interesting that the superhelical density of the DNA of prokaryotes as well as eukaryotes is very similar with a value of  $\sigma = -0.06$  in the absence of proteins (Giaever & Wang, 1988). The superhelical organization of DNA increases the contact probability of two sites up to a value of  $j_M$  around  $10^{-6}$  M as compared to the linear or open circular form (Vologodskii *et al.*, 1992).

The DNA conformation depends also on the sequence. The different molecular properties of dA·dT and dG·dC base-pairs can lead to local changes of the DNA conformation (Dickerson & Drew, 1981; Hagerman, 1990). If these deviations from the average DNA helix structure are in phase with the helical twist they can lead to significant intrinsic curvature of the DNA (Trifonov & Sussman, 1980). In particular, tracts of four to six dA residues with a periodicity of 10 to 11 base-pairs induce a strong curvature of the DNA helix axis (Diekmann & Wang, 1985; Hagerman, 1990; Trifonov & Ulanovsky, 1988; Wu & Crothers, 1984). The curvature can be predicted from the DNA sequence according to various models (Bolshoy *et al.*, 1991; Cacchione *et al.*, 1989; Calladine *et al.*, 1988; Goodsell & Dickerson, 1994; Koo & Crothers, 1988; Munteanu *et al.*, 1998; Satchwell *et al.*, 1986). In numerical simulations of linear DNA the insertion of a curved DNA region increased the value of  $j_M$  by one to two orders of magnitude for separation distances <500 base-pairs (Merlitz *et al.*, 1998; Rippe *et al.*, 1995).

A superhelical DNA conformation in conjunction with DNA curvature can be even more effective in increasing the local concentration of distant sites up to values of  $10^{-5}$  M (Klenin *et al.*, 1995). Supercoiled plasmids are flexible molecules whose shapes fluctuate and depend on experimental conditions. The presence of a permanent bend introduced by an intrinsic curved DNA sequence or a bending protein decreases the amplitude of the internal motion in superhelical plasmids and strongly organizes the superhelix structure. The bend will be found more often in the end loop of a superhelix, since these regions are more strongly bent than the rest of the plasmid. This effect has been studied both theoretically (Diekmann & Langowski, 1995; Klenin *et al.*, 1995; Wedemann *et al.*, 1998) and experimentally (Kremer *et al.*, 1993; Laundon & Griffith, 1988; Pfannschmidt & Langowski, 1998). Thus, for DNA regions located symmetrically with respect to the curved sequence, contacts should be facilitated, whereas an asymmetric location would disfavor the interaction.

Here, the effect of the DNA conformation on the transcription activation rate was studied in the NtrC/RNAP· $\sigma^{54}$  system. Plasmids with an intrinsic bend were constructed which differed in the distance of the enhancer to the promoter and the location of the bend. With these templates the transcription activation rate was analyzed in single-round transcription experiments. The activation rate is expected to depend, at least to some extent, on the contact probability between the NtrC-P complex at the enhancer and RNAP· $\sigma^{54}$  at the promoter. Therefore the results were compared with the local concentration of NtrC-P complex at the enhancer in the proximity of RNAP· $\sigma^{54}$  at the promoter as predicted from analytical calculations and numerical simulations.

## Results

### Preparation and analysis of plasmid templates

For the *in vitro* transcription experiments a number of plasmids with an intrinsically curved sequence containing six dA5/dA6 tracts between the enhancer (two strong NtrC binding sites) and the *glnAp2* promoter were constructed. The relative position of the dA tracts is referred to in the following by the quotient of the distance between the enhancer and the curved insert (center to center) divided by the distance of the enhancer to the promoter. Accordingly, a value of 0.5 would correspond to a location of the curved segment exactly in the middle between enhancer and promoter, which we will call a symmetric position. For a position of the curvature with values of 0.4 to 0.6 the corresponding plasmids were designated as CS (curvature symmetric), whereas other locations of the curvature position were indicated in the plasmid name with CA (curvature asymmetric). The subsequent two numbers in the plasmid name refer to the distance from the enhancer to the curved insert and to the distance from the curved insert to the promoter.

Figure 1 shows the predicted conformation of the enhancer-promoter region for the plasmids studied using the data set from Bolshoy *et al.* (1991) in the program CURVATURE as described by Schätz & Langowski (1997). The other algorithms (Cacchione *et al.*, 1989; Calladine *et al.*, 1988; Koo & Crothers, 1988; Satchwell *et al.*, 1986) gave similar results, although, in general, the magnitude of curvature for the dA tract was lower. For all plasmids except pVW7 and pTH8 a strong curvature of the inserted fragment is predicted between enhancer and promoter. In addition, some minor bending at other positions can be seen. In order to confirm the predicted curvature experimentally the inserted regions were cut out with *PstI* and analyzed on a native 8% (w/v) polyacrylamide gel. From the comparison with a DNA length standard the *k*-factor was determined (Table 1). The *k*-factor describes the anomalous gel mobility of a DNA fragment due to intrinsic DNA curvature and was calculated by dividing the apparent DNA length by the length known from the DNA sequence (Diekmann & Langowski, 1995). For values of  $k \approx 1$ , apparent and real sequence length are similar. The effect of the intrinsic curvature is more pronounced if the sequence is located in the center of the fragment, whereas a curvature at the end of the fragment has little effect. A value of  $k > 1.35$  is regarded as indicative of strong curvature in the middle of the fragment. This is the case for the DNAs studied here (Table 1) except for the inserts of pCS119-119, for which a somewhat lower *k*-factor of 1.19 was determined. The corresponding *PstI* fragments are relatively short (130 bp), and it appears possible that the corresponding measurement resulted in too low a *k*-value, since the DNA standard used did not cover the short DNA length

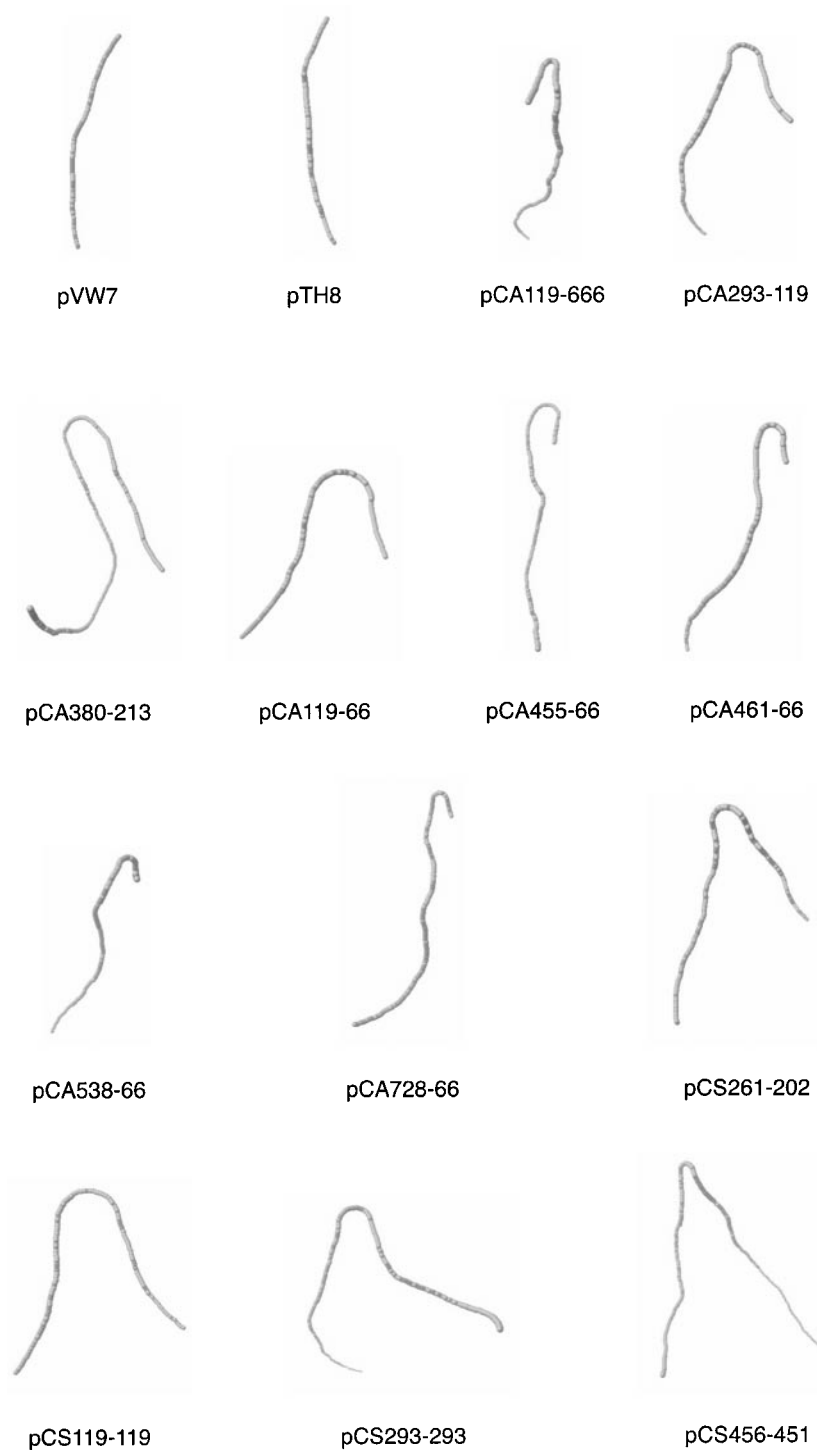


**Figure 1.** Predicted conformation of the region between enhancer and promoter. Calculations were made with the algorithm described by Bolshoy *et al.* (1991) with the program CURVATURE (Schätz & Langowski, 1997). The end with the *glnAp2* promoter is located at the top or right side and the enhancer at the bottom or left side of the images.

range (<150 bp) very well. In order to analyze the DNA curvature of the enhancer-promoter region of plasmid pTH8 it was digested with *HindIII* and *HinI*. The relevant fragment comprising the enhancer to promoter region is 215 bp long (*HinI* cut at position -200 and *HindIII* cut at position +14). This fragment moved like a 226 bp long fragment on the native polyacrylamide gel, i.e. the *k*-factor was only 1.05 and there was no indication for significant intrinsic DNA curvature consistent

with the DNA conformation predicted from the sequence (Figure 1).

After the plasmid preparations, varying amounts of superhelical plasmid monomers and dimers and the nicked/linear forms of the plasmid were detected. Since the integrity and homogeneity of the template was crucial for the experiments, the superhelical plasmid monomers were purified by agarose gel electrophoresis. The superhelical density  $\sigma$  of the plasmid preparations used is given in

**Table 1.** Intrinsic curvature of DNA sequence between enhancer and promoter

Plasmid	Position of curvature <sup>a</sup>	Sequence length (bp) <sup>b</sup>	Apparent length (bp) <sup>c</sup>	<i>k</i> -factor <sup>d</sup>
pCA119-666	0.15	677	644	0.95
pCS119-119	0.50	130	155	1.19
pCS293-293	0.50	478	699	1.46
pCS456-451	0.50	799	1275	1.60
pCS261-202	0.56	355	495	1.39
pCA380-213	0.64	485	684	1.41
pCA119-66	0.64	77	81	1.05
pCA293-119	0.71	304	391	1.29
pCA455-66	0.87	413	455	1.10
pCA461-66	0.87	419	460	1.09
pCA538-66	0.89	496	487	0.98
pCA728-66	0.92	686	625	0.91
pTH8 <sup>b</sup>	-	215	226	1.05

<sup>a</sup> The position of the curvature was defined as the center-to-center distance from the enhancer to the curved sequence divided by the distance from enhancer to promoter. A value of 0.5 would correspond to a location of the curvature in the middle between enhancer and promoter.

<sup>b</sup> This is the length of the *Pst*I fragment that contains the curved insert as well as any other sequence cloned into the region between enhancer and promoter from pVW7. For the analysis of pTH8 the plasmid was digested with *Hind*III and *Hin*fl. The relevant fragment comprising the enhancer to promoter region was 215 bp long and moved like a 226 bp long fragment on the native polyacrylamide gel.

<sup>c</sup> The apparent DNA length was determined from the gel mobility of a given fragment as compared to a standard of DNA fragments with the program Bio Image IQ version 2.1.1.

<sup>d</sup> The *k*-factor describes the anomalous gel mobility of a DNA fragment due to intrinsic DNA curvature and was calculated by dividing the apparent DNA length by the length known from the DNA sequence (Diekmann & Langowski, 1995).

Table 2. The values of  $\sigma$  for our purified superhelical templates were around  $-0.04$  to  $-0.05$ , with the amount of nicked plasmid present being  $< 5\%$ . The measured superhelical density of the templates was somewhat lower than the typical value for purified plasmids of  $\sigma = -0.06$ , but higher than the amount of unconstrained supercoiling in *E. coli* that has been estimated to be equivalent to  $\sigma = -0.03$  (Bates & Maxwell, 1993). Since the *glnAp2* promoter is relatively insensitive to the exact degree of negative supercoiling (see below), it appears unlikely that the small differences in the value of  $\sigma$  between the different templates have a significant effect on the measured activation rates.

### Transcription kinetics

The RNAP· $\sigma^{54}$  holoenzyme forms a stable closed complex at the *glnAp2* promoter in the absence of NtrC. Thus, protein binding and transcription activation can be examined separately. The transcription kinetics were conducted as described in Materials and Methods. The system consisted of the DNA template with the *glnAp2* promoter sequence and NtrC binding sites, the RNAP· $\sigma^{54}$ , and the activator protein NtrC. The necessary phosphorylation of NtrC that is performed *in vivo* by NtrB was reproduced *in vitro* with the chemical agent carbamyl phosphate (Feng *et al.*, 1992). After binding of the RNAP· $\sigma^{54}$  at the promoter and NtrC-P at the enhancer, the reaction was started by the addition of ATP. The kinetics of the activation reaction were monitored by taking samples at different times and adding them to a mix of nucleotides and heparin. Since heparin prevents the rebinding of the polymerase and destroys closed complexes, only the open complex present

at a given time-point could produce a radioactive transcript. Accordingly, the transcription activation rate with different templates could be measured by quantifying the amount of radioactive RNA transcript produced over time. In all reactions, plasmid pVW7-158 was present as an internal reference. This plasmid produced a transcript of only 158 nt from the *glnAp2* promoter as opposed to 484 nt for the other templates studied (except for pTH8, from which a 298 nt transcript is produced). The different lengths of the transcripts were accounted for by normalizing the amount of radioactive transcript with respect to the same number of C residues. Figure 2(a) shows a typical phosphorimager picture of the activation kinetics. The bottom band corresponds to the superhelical pVW7-158 reference plasmid, whereas the upper band refers to the pVW7 template linearized at the *Eco*RI restriction site upstream of the enhancer. As demonstrated by the quantitative analysis of the bands, the activation reaction of the superhelical template shows an almost linear increase for about the first two to three minutes and then reaches a plateau (Figure 2(b)). At this point probably an equilibrium between the formation and the decay of open complexes is reached, so that no more open complexes were formed. The linearized pVW7 template that had a sequence identical with that of pVW7-158 except for the longer transcript showed a much lower activation rate. Since the linear relation between the amount of transcript produced and time was only valid for the first two minutes, the transcription activation rate was determined from samples taken every ten seconds for the first 90 seconds. Representative examples for the transcription activation reaction during this time are shown in Figure 3 for different templates.

**Table 2.** Measured rates of transcription activation by NtrC

Plasmid	Total length (bp)	Distance enhancer/promoter	Curvature position <sup>a</sup>	$\sigma^b$	Activation rate <sup>c</sup>	Std. dev. <sup>d</sup>	N <sup>e</sup>
pCA119-666	3992	785	0.15	-0.042	1.36( $\pm$ 0.46)	0.67	8
pCA380-213	3800	593	0.64	-0.044	1.43( $\pm$ 0.20)	0.31	9
pCA119-66	3391	185	0.64	-0.046	1.56( $\pm$ 0.44)	0.50	5
pCA293-119	3619	413	0.71	-0.038	1.46( $\pm$ 0.34)	0.46	7
pCA455-66	3728	521	0.87	-0.045	1.11( $\pm$ 0.34)	0.49	8
pCA461-66	3734	527	0.87	-0.042	4.69( $\pm$ 1.39)	2.25	10
pCA538-66	3811	604	0.89	-0.044	0.78( $\pm$ 0.19)	0.27	8
pCA728-66	4001	794	0.92	-0.042	1.45( $\pm$ 0.37)	0.57	9
pCS119-119	3445	238	0.50	-0.046	1.54( $\pm$ 0.39)	0.66	11
pCS293-293	3793	586	0.50	-0.039	1.18( $\pm$ 0.36)	0.45	6
pCS456-451	4114	907	0.50	-0.036	1.52( $\pm$ 0.47)	0.63	7
pCS261-202	3670	463	0.56	-0.043	7.57( $\pm$ 1.77)	4.14	21
pVW7	3114	109	-	-0.057	0.97( $\pm$ 0.29)	0.49	11
pTH8	3576	109	-	-0.050	3.36( $\pm$ 1.19)	1.49	6
Linear pVW7 <sup>f</sup>	3114	109	-	-	0.04( $\pm$ 0.01)	0.00	4
Linear pTH8 <sup>f</sup>	3576	109	0.44	-	0.15( $\pm$ 0.05)	0.07	8
Linear pCS119-119 <sup>f</sup>	3445	238	0.50	-	0.18( $\pm$ 0.04)	0.05	6
Linear pCS261-202 <sup>f</sup>	3670	463	0.56	-	0.12( $\pm$ 0.02)	0.02	6
Linear pCA119-66 <sup>f</sup>	3391	185	0.64	-	0.13( $\pm$ 0.02)	0.03	6
Linear pCA293-119 <sup>f</sup>	3619	413	0.71	-	0.06( $\pm$ 0.02)	0.02	6

<sup>a</sup> The curvature position is defined as described in the legend to Table 1.

<sup>b</sup> Superhelical density of the purified plasmid preparation analyzed.

<sup>c</sup> Activation rates  $\pm$ 95% confidence interval of the mean value were determined as described in Materials and Methods.

<sup>d</sup> Standard deviation of the measured activation rates.

<sup>e</sup> Number of experiments.

<sup>f</sup> The plasmids were linearized with *EcoRI*, which is located upstream of the two strong NtrC binding sites.

The quantitative analysis of the phosphorimager data is presented in Figure 4. The transcription activation rate was obtained from the slope of a linear regression fit to a plot of the amount of transcript *versus* time. After correction for the different template length, the ratio of the transcription activation rate of pVW7 to that of pVW7-158 was determined to be 0.97( $\pm$ 0.29) (Table 2). Thus, as expected the two plasmids that differed only in the length of the RNA transcript produced, displayed essentially the same activation rate after correction for the different transcript length. This indicates that our method is suitable for an accurate determination of the transcription activation rate. The results of the transcription kinetic experiments are summarized in Table 2.

### Superhelical *versus* linear templates

The linearized plasmids displayed an activation rate that was ten- to 60-fold lower than that of the corresponding superhelical plasmids (Table 2 and 3). The presence of an intrinsically curved DNA sequence increased the activation rate of the linear templates four to five times (compare pCS119-119 with pVW7, Table 2). Within the limited data set for the linearized templates it appears that a centrally located curvature as in pCS119-119/*EcoRI* (curvature position at 0.5, activation rate 0.18( $\pm$ 0.04)) resulted in a higher activation rate than a more asymmetrically located one like that in pCS261-202/*EcoRI* (curvature position 0.56, activation rate 0.12( $\pm$ 0.02)) or in pCS293-119/*EcoRI* (curvature position 0.71, activation rate

0.06( $\pm$ 0.02)) (Table 2 and 3). Plasmid pTH8 showed a higher activation rate than pVW7 in the linearized as well as in the superhelical conformation. As discussed below, it contains three weak NtrC binding sites in addition to the two strong NtrC sites found in pVW7, which might increase the activation rate.

### Comparison of superhelical templates

The distance between enhancer and promoter had little effect on the observed activation rate (Figure 5(a)). In addition, no systematic effect for the presence and/or location of the inserted curved sequence was observed with the superhelical templates (Figure 5(a) and (b)). Most of the values were between 0.8 and 1.6 (Figure 5(b)). Only three plasmids had a significantly higher activation rate than the pVW7 reference plasmid. These were pCA461-66 (4.69( $\pm$ 1.39)), pTH8 (3.36( $\pm$ 1.19)), and pCS261-202 (7.57( $\pm$ 1.77)). However, the transcription activation rate varied up to a factor of 10 between some of the constructs. The comparison between pCA538-66 (0.78( $\pm$ 0.19)) and pCS261-202 (7.57( $\pm$ 1.77)) shows that the position of the curvature and/or the specific DNA sequence between enhancer and promoter can modulate the activation rate by an order of magnitude.

### Discussion

Transcription initiation in the NtrC/RNAP· $\sigma^{54}$  system studied here requires the transient inter-

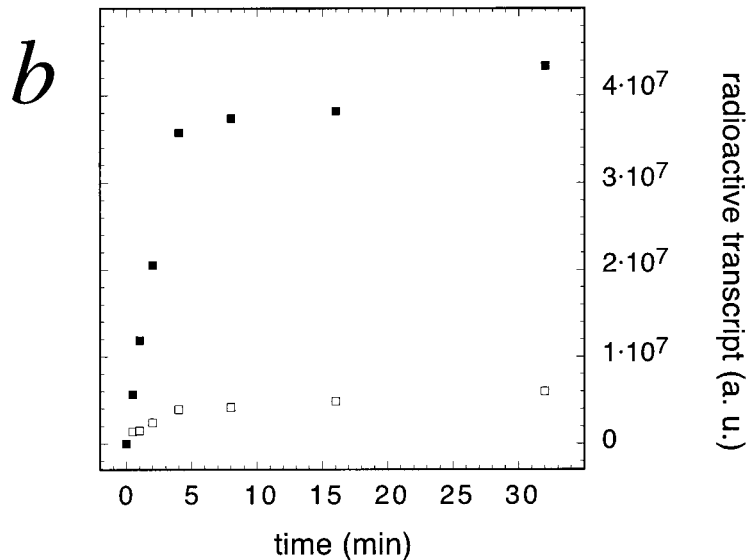
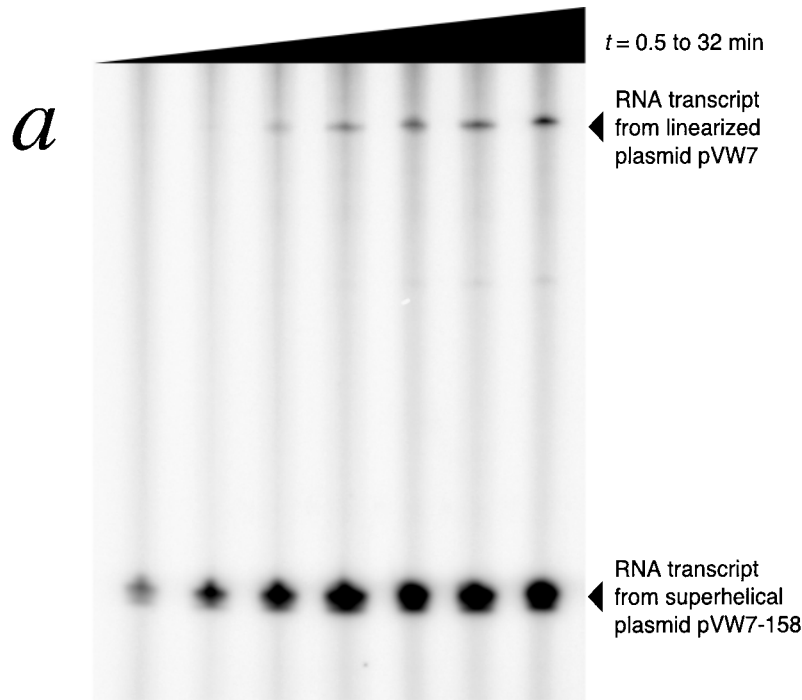


**Figure 2.** Transcription kinetic of pVW7 linearized with *EcoRI*. (a) Phosphorimager picture of the transcription kinetic of pVW7/*EcoRI* analyzed on a urea/6% polyacrylamide gel. The linearized pVW7 produced a 484 nt transcript, while the internal superhelical control plasmid pVW7-158 produced a 158 nt transcript. (b) Quantification of the amount of RNA transcript produced from: *EcoRI* linearized pVW7, (□); or the superhelical pVW7-158 reference, (■).

action of the NtrC-P complex at the enhancer with RNAP· $\sigma^{54}$  bound at the *glnAp2* promoter. The effective concentration  $c_{\text{eff}}$  of the biologically active NtrC-P complex with respect to RNAP· $\sigma^{54}$  at the promoter is given by:

$$c_{\text{eff}} = \theta_{\text{NtrC}} \times \theta_{\text{RNAP}} \times j_M + c_{\text{free}} \quad (1)$$

In equation (1)  $\theta_{\text{NtrC}}$  and  $\theta_{\text{RNAP}}$  denote the occupancy of the enhancer and the promoter, and  $c_{\text{free}}$  the concentration of non-DNA-bound NtrC-P octamer that is able to activate transcription. Under the conditions of the experiments described here the sites are fully occupied, since the concentrations of

both NtrC and RNAP· $\sigma^{54}$  have been chosen in titration experiments to give a maximal activation rate (see Materials and Methods) and to saturate the respective binding sites, i.e.  $\theta_{\text{NtrC}} = 1$  and  $\theta_{\text{RNAP}} = 1$  (see also Rippe, 2000; Schulz *et al.*, 1998). In the absence of the specific binding sites, no activation was observed and accordingly  $c_{\text{free}} \approx 0$ . Thus, the effective concentration of the NtrC-P complex is given by the local molar concentration  $j_M$  of the enhancer in the proximity of the promoter, which in turn is dependent on the DNA conformation of the template. The value of  $j_M$  has been calculated for linearized (Merlitz *et al.*, 1998;

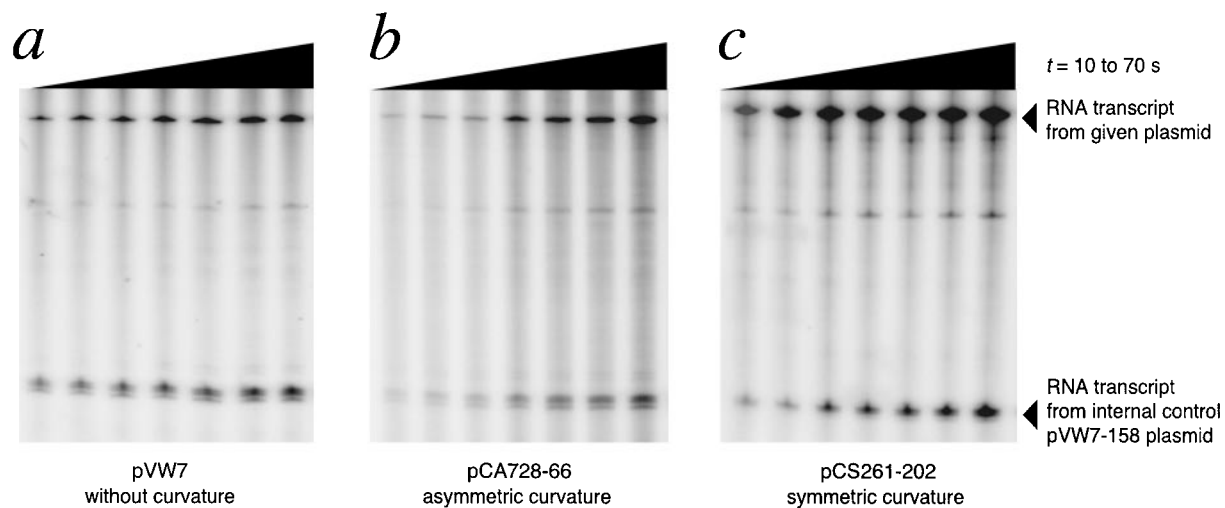


**Figure 3.** Phosphorimager images of transcription kinetics of superhelical templates. The images show the 484 nt transcript of the indicated three different superhelical plasmids and the 158 nt transcript of the internal control from pVW7-158 that is produced during the initial phase of the first 70 seconds (time-points every ten seconds). (a) pVW7, (b) pCA728-66, and (c) pCS261-202.

Rippe *et al.*, 1995) and superhelical DNAs (Klenin *et al.*, 1995; Vologodskii *et al.*, 1992), including the effect of an intrinsically curved DNA region between enhancer and promoter. To a first approximation, we expected that within a certain range a higher local concentration will result in a higher activation rate. This hypothesis was tested here. Tables 3 and 4 show a comparison between the calculated local concentration and the measured activation rate of representative plasmids.

### Superhelical versus linear templates

The superhelical templates showed a ten- to 60-fold higher activation rate than their linearized forms (Table 3). There are two effects that have to be taken into account to explain this difference: In the superhelical conformation, the interaction between enhancer and promoter is facilitated, as expected from the theoretical predictions on the contact probability, by a factor of 13 to 190 (Table 3). On the other hand, it has been reported that negative superhelicity can support the melting of the promoter DNA (Drew *et al.*, 1985; Pruss & Drlica, 1989). Since this effect is not present with the linearized plasmids, a direct comparison of superhelical and linearized templates in terms of the local concentration could be problematic. However, it has been shown that the *glnAp2* promoter studied here is relatively independent of the degree of supercoiling (Dixon *et al.*, 1988; Ninfa *et al.*, 1987; Whitehall *et al.*, 1992). In addition, studies with heteroduplex DNA templates demonstrate that RNAP- $\sigma^{54}$  requires NtrC activator protein to

initiate transcription even when the DNA in the promoter region is already in the melted conformation (Cannon *et al.*, 1999; Wedel & Kustu, 1995). It appears therefore unlikely that the strand separation of the promoter DNA is the rate-limiting step in the reaction leading to the formation of the open complex. Accordingly, the observed differences in the transcription activation rate between linear and superhelical templates should predominantly reflect differences in the contact probability between the activator complex and the polymerase.

In Table 3 the ratio of the activation rates for the six plasmids studied both in the superhelical and linearized form is compared to the corresponding ratio of the local concentration  $j_M$ . The comparison shows a qualitative agreement between experimental and theoretical values. The measured increase in the activation rate due to the formation of a superhelix was not quite as high as expected for the increase in  $j_M$  but nevertheless in the predicted range of one to two orders of magnitude. For the plasmid pTH8 a difference by a factor of  $\sim 7$  and for pVW7 by a factor  $>30$  (estimated) was observed between the superhelical and the linear template in a previous study (Carmona & Magasanik, 1996). In these experiments, the equilibrium distribution of open and closed complex obtained after incubation for 20 minutes was measured, as opposed to the transcription activation rate determined here. The difference in the results between pVW7 and pTH8 has been attributed to a  $65^\circ$  DNA bend present in pTH8 at position  $-73$  between enhancer and promoter (Carmona *et al.*, 1997; Carmona &

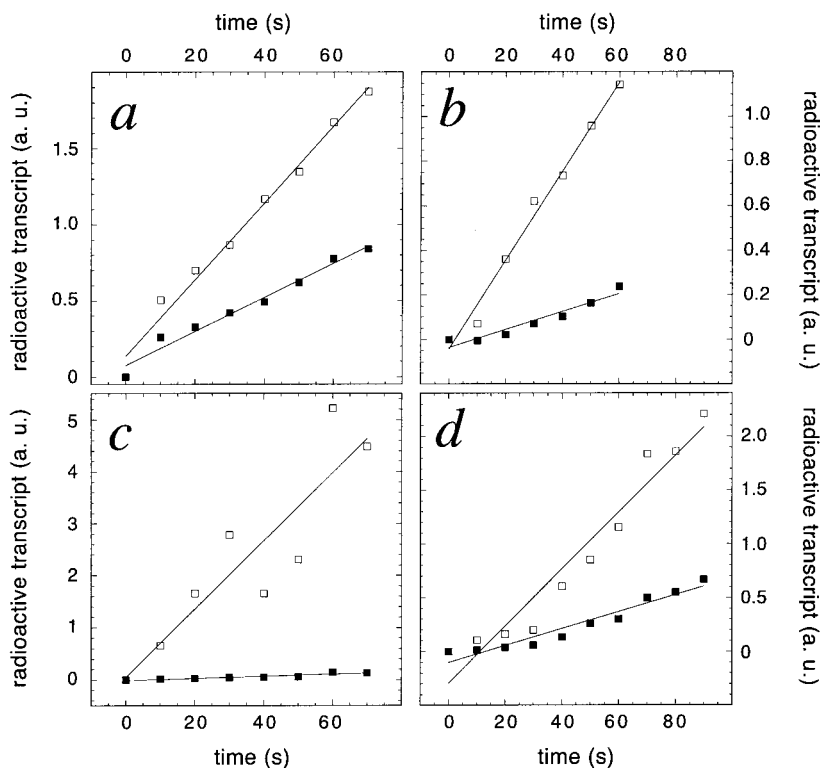


**Figure 4.** Quantitative analysis of transcription kinetics. Examples for the analysis of the phosphorimager images. The amount of radioactivity in a given band was quantitated and after subtraction of the background plotted *versus* the time allowed for open complex formation. The slope of the lines corresponds to the initial activation rate.  $\square$ , (a) pVW7, (b) pTH8, (c) pCS261-202, (d) pCA728-66;  $\blacksquare$ , (a)-(d) pVW7-158 internal reference.

Magasanik, 1996). Our gel electrophoretic analysis, however, revealed no significant intrinsic curvature for pTH8 in this region. Both pVW7 and pTH8 have the same distance between the promoter and the two strong NtrC-binding sites that constitute the minimal enhancer sequence (at  $-148$  to  $-132$  and  $-116$  to  $-100$ ). In addition, pTH8 possesses three weak NtrC binding sites upstream of the *glnAp2* promoter ( $-94$  to  $-81$ ,  $-73$  to  $-60$ , and  $-53$  to  $-37$ ). As demonstrated by fluorescence cross-correlation spectroscopy experiments, the NtrC-P octamer complex can bind two DNA strands (Rippe, 2000). As discussed by Rippe (2000), the NtrC-P complex could potentially also interact with one or two of the weaker binding sites and thereby facilitate the formation of the looped intermediate with RNAP $\cdot\sigma^{54}$ . This would explain why pTH8 displayed a higher activation rate than pVW7 both with the linearized and the superhelical template.

### Comparison of linear templates

The local concentration for linear DNA with an enhancer-promoter separation of 100 to 200 bp increased from around  $10^{-8}$  M up to  $10^{-6}$  M in the numerical simulations, when a strongly curved segment ( $120^\circ$  kink) was present in the center of the fragment (Merlitz *et al.*, 1998; Rippe *et al.*, 1995) (Figure 6(a) and (b)). The effect of the curvature was most pronounced for short separation distances and disappeared above 500 base-pairs. A curvature located at other positions (Figure 6(c)) was less effective (Merlitz *et al.*, 1998). In agree-

ment with these theoretical predictions, the linearized pCS119-119 plasmid with a short separation distance and the centrally located curved insert displayed the highest activation rate of the linear templates studied ( $0.18(\pm 0.04)$ ). For larger separation distances as in pCS261-202, the measured activation rate was lower ( $0.12(\pm 0.02)$ ). In addition, the templates with the asymmetrically located curved sequence showed the expected reduction of the activation rate as compared to the centrally positioned curvature (compare pCS119-119 with pCA119-66 and pCS261-202 with pCA293-119 in Table 3).

### Comparison of superhelical templates

Three of the plasmids examined here showed a significantly increased activation rate (pTH8  $3.36(\pm 1.19)$ ; pCA461-66  $4.69(\pm 1.39)$ ; and pCS261-202  $7.57(\pm 1.77)$ ) above the average value of the other superhelical templates of  $1.31(\pm 0.15)$ . As discussed above, the pTH8 plasmid possesses three additional weak NtrC-binding sites which might lead to a higher activation rate by stabilizing the looped complex as suggested by Rippe (2000). For the other two plasmids, differences from the rest of the plasmid templates studied are not evident. While pCS261-202 has a more or less symmetrically located curved insert this is not the case for pCA461-66. It is possible that in conjunction with additional DNA bending introduced by the binding of NtrC and/or RNAP $\cdot\sigma^{54}$  a superhelical plasmid conformation is stabilized in pCS261-202 or pCA461-66 that is favorable for the activation reac-

**Table 3.** Comparison of the activation rate of superhelical and linearized plasmids

Plasmid	Position of curvature	Superhelical	Linearized	Ratio sc/lin <sup>a</sup>	Calculated ratio of $j_M$ <sup>b</sup>
pCS119-119	0.50	1.54(±0.39)	0.18(±0.04)	9(±3)	90
pCS261-202	0.56	7.57(±1.77)	0.12(±0.02)	63(±18)	190
pCA119-66	0.64	1.56(±0.44)	0.13(±0.02)	12(±4)	13
pCA293-119	0.71	1.46(±0.34)	0.06(±0.02)	24(±10)	15
pVW7	-	0.97(±0.29)	0.04(±0.01)	25(±10)	100
pTH8	-	3.36(±1.19)	0.15(±0.05)	22(±11)	100

<sup>a</sup> Ratio of transcription activation rates of superhelical template (sc) to the linearized (lin) form.

<sup>b</sup> Calculated ratio of the local concentration for the enhancer/promoter interactions for superhelical and linear templates.

tion. As inferred from scanning force microscopy images, RNAP· $\sigma^{54}$  bends the *glnAp2* promoter in the closed complex by about 30-50° (Rippe *et al.*, 1997; Schulz *et al.*, 1998). The NtrC-P complex at the enhancer, on the other hand, apparently also induces significant bending of the enhancer DNA (Fiedler, 1996; Révet *et al.*, 1995). In addition, the particular sequences introduced between the enhancer and promoter in pCS261-202 and pCA461-66 might facilitate the activation reaction. Additional experiments are necessary to determine the reason for the increased activation rate observed with these templates. At this point we can only note that the activation rates determined with pCS261-202 are up to ten times higher than that of other templates studied (e.g. pCA538-66, 0.78(±0.19)). This demonstrates that a specific DNA sequence between the enhancer and promoter region can lead to a large increase of the activation reaction of the superhelical templates.

No systematic differences were found for the superhelical plasmids studied both with respect to the distance between enhancer and promoter as well as the location of the curved insert. Except for the two templates pCS261-202 and pCA461-66 discussed above, the activation rate was remarkably

insensitive with respect to the distance between enhancer and promoter as well as the location of the curved insert with an average value of 1.31(±0.15). The relative insensitivity of the superhelical templates to the distance between enhancer and promoter is expected from the numerical simulations. Variation of the separation distance from 300 to 2000 bp did not lead to significant changes of the calculated  $j_M$  value of  $6 \times 10^{-6}$  M (Klenin *et al.*, 1995; Rippe *et al.*, 1995; Vologodskii *et al.*, 1992). This is in agreement with previous *in vivo* studies with plasmid templates without curvature where little effect on the production of glutamine synthetase was detected if the distance between enhancer and promoter was expanded to 3000 bp (Reitzer & Magasanik, 1986; Reitzer *et al.*, 1989).

#### Effect of curvature with superhelical templates

An increasing local concentration has been calculated for superhelical plasmids with symmetric curvature *versus* plasmids with asymmetric curvature (Klenin *et al.*, 1995). Figure 7 schematically depicts the effect of intrinsic DNA curvature on the conformation of a superhelical plasmid. Since the

**Table 4.** Comparison of the calculated local concentration for representative templates with the measured transcription activation rates

DNA template	~200 bp distance		~500 bp distance		~1000 bp distance	
	$j_M$ (μM) <sup>a</sup>	Activation rate <sup>b</sup>	$j_M$ (μM) <sup>a</sup>	Activation rate <sup>b</sup>	$j_M$ (μM) <sup>a</sup>	Activation rate <sup>b</sup>
Linear	0.01	0.04(±0.01)	0.12	n.d.	0.07	n.d.
Linear with central curvature	0.9	0.18(±0.04)	0.3	0.12(±0.02)	0.1	n.d.
Linear with non-central curvature	0.3	0.13(±0.02)	0.2	0.06(±0.02)	0.1	n.d.
Superhelical	1	0.97(±0.29)	6	n.d.	6	n.d.
Superhelical with central curvature	80	1.54(±0.39)	60	1.18(±0.36)	40	1.52(±0.47)
Superhelical, non-central curvature	4	1.56(±0.44)	3	1.11(±0.34)	2	1.45(±0.57)
		pCS119-66		pCA455-66		pCA728-66

n.d., not determined.

<sup>a</sup> Calculated local concentration for the different DNA templates.

<sup>b</sup> Measured transcription activation rates relative to that of pVW7-158.

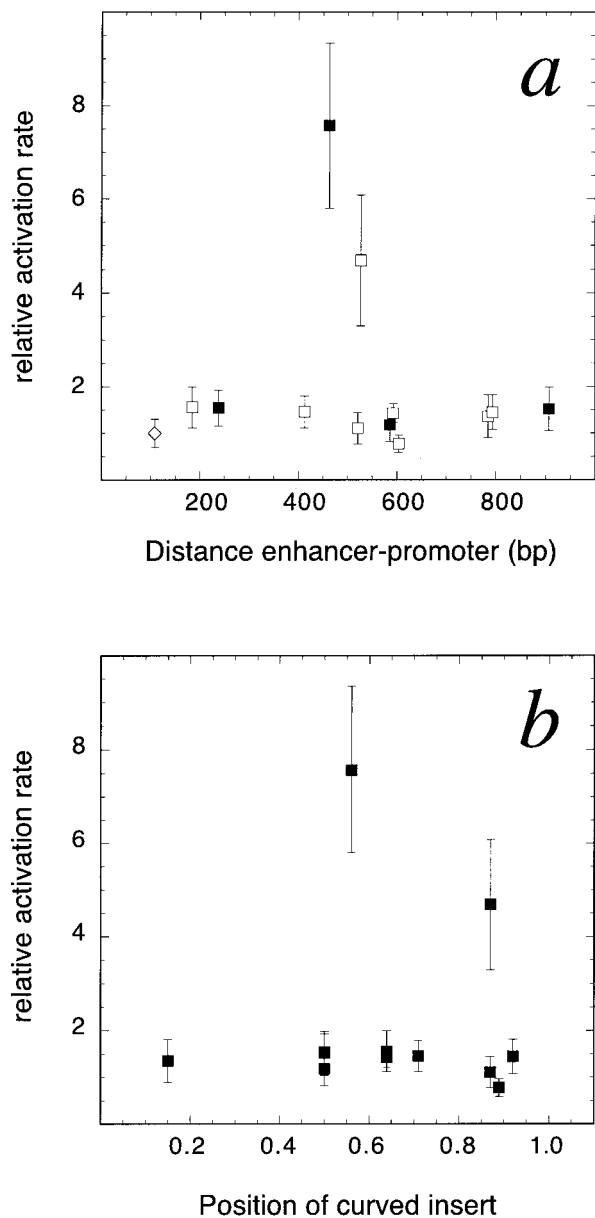


**Figure 5.** Transcription activation rates of superhelical templates. The relative activation rate is given as the ratio to the activation rate of pVW7-158, which was included in all reactions as an internal reference. Plasmid pTH8 is not shown on the plots, since it contains three additional weak NtrC binding sites, which might affect the activation rate. Only two plasmids (pCS261-202 and pCA461-66) displayed an activation rate significantly above the average. (a) Dependence of the activation rate on the distance between enhancer and promoter. Plasmids with symmetric curvature (■); plasmids with asymmetric curvature (□); plasmids without curvature (◇); are shown. (b) Dependence of the activation rate on the position of the curvature. Only two plasmids (pCS261-202 and pCA461-66) displayed an activation rate significantly above the average.

curved sequence is preferably located in the end-loop of the plasmid, a location of the curvature right in the middle between enhancer and promo-

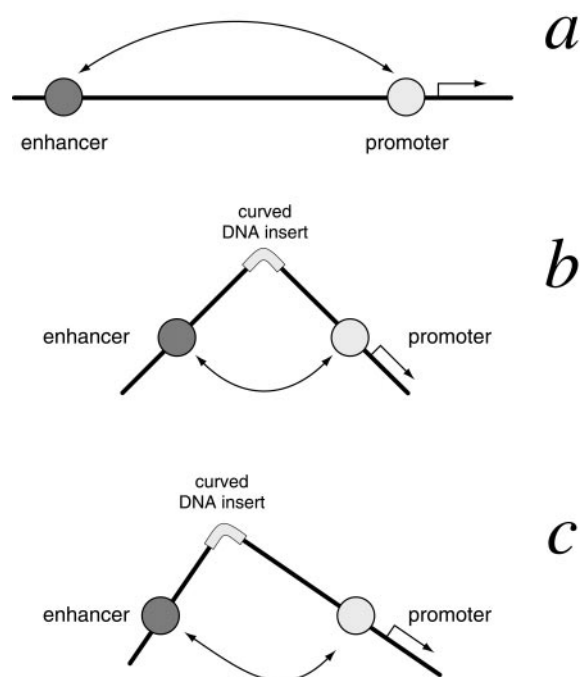


**Figure 6.** Scheme for looping-mediated interactions on linear templates. The proteins at the enhancer and the promoter are shown as gray circles; the curved insert is highlighted by gray shading. (a) Linear DNA. (b) Linear DNA with symmetric curvature. (c) Linear DNA with asymmetric curvature.

ter is predicted to facilitate interactions between enhancer and promoter (Figure 7(b)). On the other hand, the local concentration decreases with a non-central curvature (Figure 7(c)) by more than one order of magnitude from a maximum around  $7 \times 10^{-5}$  M to about  $1 \times 10^{-6}$  M for separation distances of around 300 to 700 bp (Klenin *et al.*, 1995). A corresponding change of the measured transcription activation rate was not observed in the experiments. Thus, an increase of the local concentration  $j_M$  above  $\sim 10^{-6}$  M by inserting a curved DNA segment between enhancer and promoter did have no significant effect on the transcription activation rate in the system studied here.

Curvature of the DNA between enhancer and promoter can also be introduced by a protein like IHF (integration host factor) that bends the DNA upon binding by about  $160^\circ$  (Ellenberger & Landy, 1997; Rice, 1997; Rice *et al.*, 1996). The IHF-mediated bending can facilitate the contact between NtrC-P or related activators like NifA and RNAP $\cdot\sigma^{54}$  bound to their respective sites (Claverie-Martin & Magasanik, 1992; Hoover *et al.*, 1990; Molina-López *et al.*, 1994; Santero *et al.*, 1992). It has also been reported recently that IHF directly increases the binding of RNAP $\cdot\sigma^{54}$  to the *Pu* promoter of *Pseudomonas putida* (Carmona *et al.*, 1999) which indicates an additional activity of IHF. However, since the effect of IHF binding can be substituted by an intrinsically curved DNA

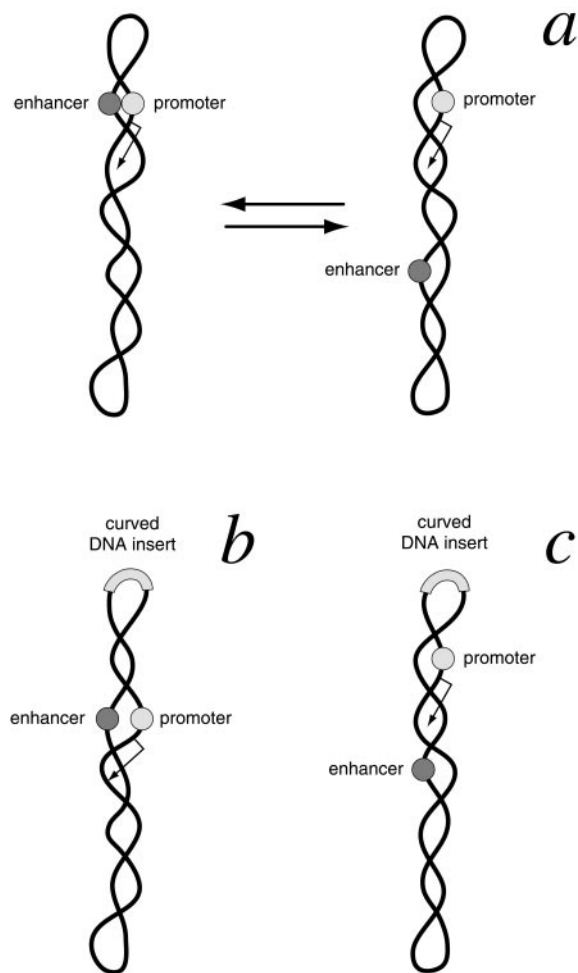


**Figure 7.** Scheme for looping-mediated interactions on superhelical templates. The proteins at the enhancer and the promoter are shown as gray circles; the curved insert is highlighted by gray shading. (a) Superhelical plasmid without intrinsic curvature. All conformations are equally probable as indicated by the equilibrium between a conformation in which enhancer and promoter are in close contact (left side) and a conformation in which they are further apart (right side). Due to slithering of the two DNA strands in the superhelix there is a fast exchange between the different conformations so that enhancer and promoter are brought in contact with each other, which leads to an increase of the local concentration as compared to the linearized form. (b) Superhelical plasmids with symmetric curvature. The insert is preferably located in the end-loop so that a plasmid conformation is favored in which proteins at the enhancer and the promoter can contact each other. (c) Superhelical plasmid with asymmetric curvature. The curved insert stabilizes a plasmid conformation in which enhancer and promoter are not in close contact.

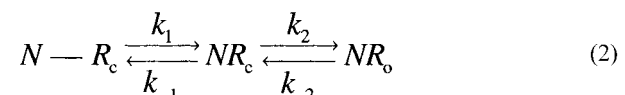
sequence at the *Klebsiella pneumoniae nifH* promoter so that 70% of the wild-type expression level is restored (Molina-López *et al.*, 1994), the predominant role of IHF binding appears to be the stabilization of a specific DNA conformation. Inasmuch as this is the case, the effect of IHF binding is similar

to the introduction of the curved A-tract between enhancer and promoter described here. It has been shown previously that binding of IHF to a site immediately upstream of the *glnHp2* promoter enhances the catalysis of RNAP· $\sigma^{54}$  open complex formation by NtrC-P with superhelical templates about twofold and that IHF binding is essential for the activation reaction on linear templates (Claverie-Martin & Magasanik, 1991, 1992). However, the NtrC-P activated initiation of transcription on superhelical templates became independent of IHF when a mutant *glnHp2* promoter with increased affinity for RNAP· $\sigma^{54}$  was used (Claverie-Martin & Magasanik, 1992). The same effect was observed for the formation of open transcription complexes at the *nifH* promoter of *K. pneumoniae* on supercoiled DNA that required the activator protein NifA and showed a 20-fold stimulation by IHF (Hoover *et al.*, 1990; Santero *et al.*, 1992). If the NifA-binding sites were replaced by NtrC binding sites, NtrC-mediated transcription was stimulated also 20-fold. Again, the effect of IHF was strongly reduced if the wild-type promoter was replaced by one with a stronger affinity for RNAP· $\sigma^{54}$ . For IHF-independent transcription it has been reported for the weak affinity *nifL* promoter (Carmona *et al.*, 1997; Whitehall *et al.*, 1992) that sequence-induced curvature due to the presence of dA tracts between enhancer and promoter can increase NtrC-P-activated transcription *in vivo* from superhelical templates about threefold (Cheema *et al.*, 1999). Thus, several lines of evidence indicate that IHF-induced or intrinsic DNA curvature exert a positive effect on transcription from superhelical templates only with promoters that have a relatively low affinity for RNAP· $\sigma^{54}$ .

With linear templates, however, different results were obtained. In the case of *glnHp2*, the initiation of transcription on linear DNA required the presence of IHF even when the promoter was replaced with a promoter that has exceptionally high affinity for RNAP· $\sigma^{54}$  (Carmona & Magasanik, 1996; Claverie-Martin & Magasanik, 1992). In a similar way in the experiments described here, the transcription activation rate was increased about four- to fivefold on linear templates if a curved DNA sequence was inserted between the strong *glnAp2* promoter and the enhancer sequence (compare for example pCS119-119 with pVW7, Table 2), whereas the difference in the superhelical conformation was within the error of the measurement.

### Model for the kinetics of open complex formation

The first steps in the activation reaction can be described by the scheme shown in equation (2):



The complex of NtrC-P at the enhancer and RNAP· $\sigma^{54}$  at the promoter, abbreviated as  $N-R_c$  forms the loop complex  $NR_c$  in which the two proteins contact each other. In this conformation NtrC-P can catalyze the isomerisation of RNAP· $\sigma^{54}$  from the closed complex  $R_c$  to the open complex  $R_o$  upon hydrolysis of ATP, so that the  $NR_o$  loop complex forms. An increase of the local concentration is expected to affect the first step of the reaction, inasmuch as it favors the formation of the  $NR_c$  species. Numerical simulations of the kinetics of the loop-formation suggest that the equilibrium between  $N-R_c$  and  $NR_o$  should be established in the millisecond time-scale, i.e. with  $k_1$  between  $10^2$  to  $10^3$  s $^{-1}$  (Jian *et al.*, 1998; Merlitz *et al.*, 1998). Thus, the initial activation rate measured here is equal to the product of the  $NR_c$  concentration and the rate  $k_2$ . If the local concentration of NtrC-P is significantly higher than the equilibrium dissociation constant  $K_d$  for the bimolecular interaction between the NtrC-P complex and RNAP· $\sigma^{54}$  in the absence of DNA-looping, any further increase of  $j_M$  will have little effect, and the conversion from  $NR_c$  to  $NR_o$  will become the rate-limiting step of the reaction. Based on fluorescence measurements we estimate that this dissociation constant  $K_d$  is of the order of  $10^{-7}$  M under the conditions of the experiments (J. F. Kepert & K. R., unpublished results). With this affinity between NtrC-P and the polymerase, any template conformation with a local concentration of  $j_M < 10^{-8}$  M should be very inefficient for the activation reaction, since the separated  $N-R_c$  conformation is favored over contacts between NtrC-P and RNAP· $\sigma^{54}$ . In the absence of protein-protein interactions stabilizing the  $NR_c$  conformation,  $k_{-1}$  would be in the range of  $10^5$  to  $10^7$  s $^{-1}$  as deduced from Brownian dynamics simulation of superhelical and linear DNAs, yielding values of  $K_1 = k_1/k_{-1}$  between  $10^{-4}$  and  $5 \times 10^{-3}$  (Jian *et al.*, 1998; Merlitz *et al.*, 1998). In agreement with this prediction, the linearized pVW7 plasmid with a calculated value of  $j_M = 10^{-8}$  M displayed a very low activation rate that was near the detection limit. For the templates with local concentrations from  $10^{-8}$  M up to  $10^{-6}$  M, a good correlation with the measured activation rates was observed. In this range, a higher  $j_M$  will increase the amount of  $NR_c$  formed in step 1. However, for  $j_M \geq 10^{-6}$  M (all superhelical templates) the transcription activation rate becomes essentially independent of the interaction probability. At local concentrations this high, the equilibrium in the first step of the reaction depicted in equation (2) has shifted almost completely from the separated  $N-R_c$  form to the looped conformation  $NR_c$ . Under this condition, the conversion from the closed complex  $NR_c$  to the open complex  $NR_o$  is likely to determine the activation rate.

If we assume that at equilibrium about 50% of the superhelical pVW7 template (equivalent to a concentration of 2.5 nM in the experiments described here) have the RNA polymerase in the

open complex conformation (Wedel & Kustu, 1995), we can estimate from the type of experiments shown in Figure 2 that open complexes form with this template at an initial rate of  $d[NR_o]/dt = 1.3 \times 10^{-11}$  M s $^{-1}$ . This corresponds to a value of  $k_2$  of  $2.6(\pm 0.6) \times 10^{-3}$  s $^{-1}$  for an initial concentration of  $NR_c = 5$  nM. A similar rate constant has been determined for the decay of open complexes at the *glnAp2* promoter (plasmid pTH8) with values of  $3 \times 10^{-3}$  s $^{-1}$  (supercoiled templates, half-life eight minutes) and  $5 \times 10^{-3}$  s $^{-1}$  (linear templates, half-life  $\approx 150$  seconds) (Carmona & Magasanik, 1996). The rate constant for this process (equivalent to  $k_{-2}$  plus any contribution from non-looped open complexes) should have the same numerical value as  $k_2$ , if at equilibrium closed and open complexes are present in a 1:1 ratio. The two superhelical plasmids that displayed an activation rate above the average (pCS261-202 and pCA461-66) might adopt a favorable conformation for the second step of the reaction, i.e. have a higher  $k_2$  rate with values of  $20(\pm 5) \times 10^{-3}$  s $^{-1}$  and  $12(\pm 4) \times 10^{-3}$  s $^{-1}$ , respectively. If low-affinity promoters like *nifH* or *nifL* instead of *glnAp2* are used, as in the experiments discussed above, the occupancy of the promoter is reduced so that  $\theta_{RNAP} < 1$  and the effective concentration  $c_{eff}$  of NtrC-P is no longer equal to  $j_M$  (see equation (3)). In this situation, the formation of the looped  $NR_c$  complex can become the rate-limiting step also with superhelical templates, even if  $j_M$  is  $10^{-6}$  M, since  $c_{eff} < j_M$ . An increase of  $j_M$  by intrinsic or protein-induced DNA curvature could now facilitate the binding of RNAP· $\sigma^{54}$ , so that the promoter becomes fully saturated with the polymerase and the maximal rate of transcription is achieved. Thus, in addition to catalyzing the conversion of RNAP· $\sigma^{54}$  from the closed to the open complex, the NtrC-P activator at the enhancer would have an additional "recruitment" function for weak promoters that is similar to the proposed mechanism by which eukaryotic transcription activator proteins exert their biological function (Ptashne & Gann, 1997).

## Materials and Methods

### Protein preparation

Expression and purification of His-tagged NtrC from pNTRC-3 and His-tagged  $\sigma^{54}$  protein from pS54-2 was done according to the procedure described by Rippe *et al.* (1997, 1998). RNA polymerase core enzyme from *E. coli* was purchased from Epicentre Technologies (Madison, WI, USA). It was mixed with  $\sigma^{54}$  in a ratio of 1:2.5 to form the RNA polymerase holoenzyme at a stock concentration of  $\approx 1$   $\mu$ M.

### Construction of transcription templates

An intrinsically curved insert (77 bp) was formed by hybridizing the two oligonucleotides with the sequence

5'-GTA TCG ATA AAA AAT ATA TAA AAA TCT CTA AAA AAT ATA TAA AAA TCT CTA AAA AAT ATA TAA AAA TCG GAA CTG CA-3' and 5'-GTT CGA ATT TTT ATA TAT TTT TTA GAG ATT TTT ATA TAT TTT TTA GAG ATT TTT ATA TAT TTT TTA TCG ATA CTG CA-3'. This sequence was cloned into the single *PstI* site of pVW7 (Weiss *et al.*, 1992). The resulting plasmid pCA119-66 had the curved insert flanked by the new restriction sites for *Clal* and *BstBI* (underlined) that were introduced for the construction of plasmids with different distances of the enhancer and promoter relative to the curved insert. At the ends of the 77 bp oligonucleotide two *PstI* sites were retained which were used to check the length of the fragment after every new insertion of DNA and to determine the electrophoretic mobility (see below).

Fragments from a digestion of pUC18 with *HinP1I* were cloned into the *Clal* site of pCA119-66 yielding pCA455-66, pCA461-66, pCA538-66, and pCA728-66 or into the *BstBI* site to create pCA119-666. Plasmids pCS261-202 and pCA380-213 were constructed by ligating fragments of a digestion of pUC18 with *HinP1I* into the *Clal* site of pCA119-66 and fragments of a digestion of pET15b with *HpaII* into the *BstBI* site. The plasmid pCS119-119 was constructed by cloning a 53 bp random oligonucleotide sequence into the *BstBI* site of pCA119-66. Fragments from pUC18 digested with *HinP1I* were inserted into the *Clal* site and the *BstBI* site of pCS119-119 to construct pCS293-293 (174 bp *HinP1I* fragment into both sites) and pCS456-451 (332 bp *HinP1I* fragment into *Clal* site, 337 bp *HinP1I* fragment into *BstBI* site). The reference plasmid pVW7-158 was made by removing 326 bp from the transcription region of pVW7 using *BsaAI* and *BstDSI*. The sequence of the region between the two NtrC binding sites and the *glnAp2* promoter was confirmed by DNA sequencing for all plasmids studied.

### Plasmid characterization

The DNA curvature from the beginning of the enhancer to the end of the promoter was analyzed with the program CURVATURE (Schätz & Langowski, 1997) which is based on the Bolshoy algorithm (Bolshoy *et al.*, 1991). This region was also examined by electrophoresis of a *PstI* digest of every plasmid on a native 8% (w/v) polyacrylamide gel. From the comparison of the position of the insert-containing fragment with a DNA length standard the *k*-factor was calculated to quantify the degree of curvature (Diekmann & Langowski, 1995).

After plasmid isolation, varying amounts of plasmid dimers were present in addition to the monomeric forms. In order to obtain comparable and homogeneous template preparations the plasmid monomers were purified using the gel extraction kit from QIAGEN (Hilden, Germany).

The superhelix density of the plasmids was determined on chloroquine gels. Plasmid pVW7 (30 µg) was incubated with 25 units of topoisomerase I and 0 to 8 µl of 10 mg/ml ethidium bromide in a total volume of 30 µl of topoisomerase buffer (35 mM Tris-HCl (pH 7.5), 5 mM MgCl<sub>2</sub>, 72 mM KCl, 5 mM DTT, supplemented with 200 µg/ml BSA; aliquots of 10 × buffer were stored at -20°C and were used only once). The reaction was carried out overnight and stopped by phenol-extraction. The topoisomer distributions of the plasmids were

analyzed with respect to the pVW7 standard on a chloroquine-containing gel.

### In vitro transcription assay

For the *in vitro* transcription experiments a solution of 50 nM RNAP · σ<sup>54</sup>, 50 nM wt-NtrC dimer, 5 nM reference plasmid pVW7-158, and 5 nM the given test plasmid in HS-buffer (20 mM Hepes/KOH (pH 8.0), 10 mM Mg-acetate, 50 mM K-acetate, 1 mM DTT, and 0.1 mg/ml BSA) were incubated for five minutes at 37°C. Carbamyl phosphate was added to a final concentration of 20 mM and the samples were incubated for another five minutes. The activation reaction was started by addition of ATP to a 5 mM concentration. Every ten seconds a nucleotide chasing mix was added to a 5 µl sample of the activation reaction adding nucleotides and heparin to a final concentration of 500 nM GTP, 500 nM UTP, 23 nM CTP and 25 µg/ml of heparin, and contained 90 kBq of [α-<sup>32</sup>P]CTP.

After a ten minute incubation the chasing reaction was stopped by adding 10 µl of formamide stop solution to the reaction. The transcripts were analyzed on 6% polyacrylamide gels (19:1 (w/w) acrylamide/bis-acrylamide) with 8 M urea, visualized by autoradiography, and quantified with a phosphorimager and the computer program ImageQuant v. 1.2 (Molecular Dynamics, Krefeld, Germany). The experiments were repeated four to 21 times for every template. The activation rate was determined from the slope of a linear regression of a plot with the program Kaleidagraph v. 3.08 (Synergy Software, PA, USA). The examined plasmid and the control plasmid pVW7-158 differ in the number of C bases in the transcribed sequence (119 versus 43, pTH8: 76). To normalize the measured RNA production rate to the same transcript length, a correction factor of 2.77 (pTH8: 1.77) was used.

### Calculation of the local concentration $j_M$

For the calculations it was assumed that the enhancer and the promoter have to approach each other to within 10 nm to allow interaction between the DNA-bound proteins. The curvature introduced by the insert with the five dA tracts was estimated to be around 90°. The value of  $j_M$  in dependence of the separation distance given in base-pairs (*b*) for the different DNA templates for linearized DNAs was calculated according to equation (3) with *d* = 30 (no curvature), *d* = 150 (asymmetric 90° curvature) and *d* = 600 (central 90° curvature):

$$j_M(b) = 2.7 \times 10^{-3} \times b^{-\frac{3}{2}} \times \exp\left(\frac{(d-460)}{2.7 \times 10^{-3} \times b^2 + d}\right) \left[\frac{\text{mol}}{\text{liter}}\right] \quad (3)$$

Equation (3) has been derived from a numerical fit of the data given by Merlitz *et al.* (1998) and Rippe *et al.* (1995) using the numerical approximation derived by Ringrose *et al.* (1999) with a statistical segment length of 100 nm (equivalent to a persistence length of 50 nm). For the superhelical DNA templates with and without curvature the theoretical values of  $j_M$  were derived from the results of the Monte Carlo simulations (Klenin *et al.*, 1995; Vologodskii *et al.*, 1992).

## Acknowledgments

We thank Andreas Hunziker for sequencing the transcription templates and Verena Weiss for providing the pVW7 and pTH8 templates. K. R. thanks Peter von Hippel for help and discussions in the initial phase of the project. This work was supported by DFG grant Ri 828/1.

## References

- Bates, A. D. & Maxwell, A. (1993). *DNA Topology*, Oxford University Press, Oxford.
- Bellomy, G. R. & Record, M. T., Jr (1990). Stable DNA loops *in vivo* and *in vitro*: roles in gene regulation at a distance and in biophysical characterization of DNA. *Prog. Nucl. Acids Res.* **39**, 81-128.
- Blackwood, E. M. & Kadonaga, J. T. (1998). Going the distance: a current view of enhancer action. *Science*, **281**, 61-63.
- Bolshoy, A., McNamara, P., Harrington, R. E. & Trifonov, E. N. (1991). Curved DNA without A-A: experimental estimation of all 16 DNA wedge angles. *Proc. Natl Acad. Sci. USA*, **88**, 2312-2316.
- Buck, M., Miller, S., Drummond, M. & Dixon, R. (1986). Upstream activator sequences are present in the promoters of nitrogen fixation genes. *Nature*, **320**, 374-378.
- Cacchione, S., de Santis, P., Foti, D., Leoni, L., Palleschi, A., Risuleo, G. & Savino, M. (1989). Theoretical prediction of sequence dependent DNA superstructure and their gel electrophoresis behavior. *Biochemistry*, **28**, 8706-8713.
- Calladine, C. R., Drew, H. R. & McCall, M. J. (1988). The intrinsic curvature of DNA in solution. *J. Mol. Biol.* **201**, 127-137.
- Cannon, W., Gallegos, M. T., Casaz, P. & Buck, M. (1999). Amino-terminal sequences of sigmaN (sigma54) inhibit RNA polymerase isomerization. *Genes Dev.* **13**, 357-370.
- Carey, M. (1998). The enhanceosome and transcriptional synergy. *Cell*, **92**, 5-8.
- Carmona, M. & Magasanik, B. (1996). Activation of transcription of  $\sigma^{54}$ -dependent promoters on linear templates requires intrinsic or induced bending of the DNA. *J. Mol. Biol.* **261**, 348-356.
- Carmona, M., Claverie-Martin, F. & Magasanik, B. (1997). DNA bending and the initiation of transcription at  $\sigma^{54}$ -dependent bacterial promoters. *Proc. Natl Acad. Sci. USA*, **94**, 9568-9572.
- Carmona, M., de Lorenzo, V. & Bertonni, G. (1999). Recruitment of RNA polymerase is a rate-limiting step for the activation of the sigma(54) promoter Pu of *Pseudomonas putida*. *J. Biol. Chem.* **274**, 33790-33794.
- Cheema, A. K., Choudhury, N. R. & Das, H. K. (1999). A and T-tract-mediated intrinsic curvature in native DNA between the binding site of the upstream activator NtrC and the nifLA promoter of *Klebsiella pneumoniae* facilitates transcription. *J. Bacteriol.* **181**, 5296-5302.
- Claverie-Martin, F. & Magasanik, B. (1991). Role of integration host factor in the regulation of the glnHp2 promoter of *Escherichia coli*. *Proc. Natl Acad. Sci. USA*, **88**, 1631-1635.
- Claverie-Martin, F. & Magasanik, B. (1992). Positive and negative effects of DNA bending on activation of transcription from a distant site. *J. Mol. Biol.* **227**, 996-1008.
- Crothers, D. M., Drak, J., Kahn, J. D. & Levene, S. D. (1992). DNA bending, flexibility, and helical repeat by cyclization kinetics. *Methods Enzymol.* **212**, 3-29.
- Dickerson, R. E. & Drew, H. R. (1981). Structure of a B-DNA dodecamer. II. Influence of base sequence on helix structure. *J. Mol. Biol.* **149**, 761-786.
- Diekmann, S. & Langowski, J. (1995). Supercoiling couples DNA curvature to the overall shape and the internal motion of the DNA molecule in solution. *Theochemistry*, **336**, 227-234.
- Diekmann, S. & Wang, J. C. (1985). On the sequence determinants and flexibility of the kinetoplast DNA fragment with abnormal gel electrophoretic mobilities. *J. Mol. Biol.* **186**, 1-11.
- Dixon, R. A., Henderson, N. C. & Austin, S. (1988). DNA supercoiling and aerobic regulation of transcription from the *Klebsiella pneumoniae* nifLA promoter. *Nucl. Acids Res.* **16**, 9933-9946.
- Drew, H. R., Weeks, J. R. & Travers, A. A. (1985). Negative supercoiling induces spontaneous unwinding of a bacterial promoter. *EMBO J.* **4**, 1025-1032.
- Dunaway, M. & Dröge, P. (1989). Transcription of the *Xenopus* rRNA gene promoter by its enhancer. *Nature*, **341**, 657-659.
- Ellenberger, T. & Landy, A. (1997). A good turn for DNA: the structure of integration host factor bound to DNA. *Structure*, **5**, 153-157.
- Feng, J., Atkinson, M. R., McCleary, W., Stock, J. B., Wanner, B. L. & Ninfa, A. J. (1992). Role of phosphorylated metabolic intermediates in the regulation of glutamine synthetase synthesis in *Escherichia coli*. *J. Bacteriol.* **174**, 6061-6070.
- Fiedler, U. (1996). Der Aktivierungsmechanismus des Responseregulators NtrC, PhD thesis, University of Konstanz.
- Giaever, G. N. & Wang, J. C. (1988). Supercoiling of intracellular DNA can occur in eukaryotic cells. *Cell*, **2**, 849-856.
- Goodsell, D. S. & Dickerson, R. E. (1994). Bending and curvature calculations in B-DNA. *Nucl. Acids Res.* **22**, 5497-5503.
- Gralla, J. D. & Collado-Vides, J. (1996). Organization and function of transcription regulatory elements. In *Escherichia coli and Salmonella* (Neidhardt, F. C., ed.), vol. 1, pp. 1232-1245, ASM Press, Washington, DC.
- Hagerman, P. J. (1990). Sequence directed curvature of DNA. *Annu. Rev. Biochem.* **59**, 755-781.
- Hagerman, P. J. & Ramadevi, V. A. (1990a). Application of the method of phage T4 DNA ligase catalyzed ring-closure to the study of DNA structure. I. Computational analysis. *J. Mol. Biol.* **212**, 351-362.
- Hagerman, P. J. & Ramadevi, V. A. (1990b). Application of the method of phage T4 DNA ligase catalyzed ring-closure to the study of DNA structure. II. NaCl dependence of DNA flexibility and helical repeat. *J. Mol. Biol.* **212**, 363-376.
- Hoover, T. R., Santero, E., Porter, S. & Kustu, S. (1990). The integration host factor stimulates interaction of RNA polymerase with NIFA, the transcriptional activator for nitrogen fixation operons. *Cell*, **63**, 11-22.
- Jacobson, H. & Stockmayer, W. H. (1950). Intramolecular reaction in polycondensations. I. The theory of linear systems. *J. Chem. Phys.* **18**, 1600-1606.
- Jian, H., Schlick, T. & Vologodskii, A. (1998). Internal motion of supercoiled DNA: Brownian dynamics

- simulations of site juxtaposition. *J. Mol. Biol.* **284**, 287-296.
- Klenin, K. V., Frank-Kamenetskii, M. D. & Langowski, J. (1995). Modulation of intramolecular interactions in superhelical DNA by curved sequences: a Monte Carlo simulation study. *Biophys. J.* **68**, 81-88.
- Koo, H.-S. & Crothers, D. M. (1988). Calibration of DNA curvature and a unified description of sequence-directed bending. *Proc. Natl Acad. Sci. USA*, **85**, 1763-1767.
- Kremer, W., Klenin, K., Diekmann, S. & Langowski, J. (1993). DNA curvature influences the internal motions of supercoiled DNA. *EMBO J.* **12**, 4407-4412.
- Laundon, C. H. & Griffith, J. D. (1988). Curved helix segments can uniquely orient the topology of super-twisted DNA. *Cell*, **52**, 545-549.
- Magasanik, B. (1996). Regulation of nitrogen utilization. In *Escherichia coli and Salmonella* (Neidhardt, F. C., ed.), vol. 1, pp. 1344-1356, ASM Press, Washington, DC.
- Merlitz, H., Rippe, K., Klenin, K. V. & Langowski, J. (1998). Looping dynamics of linear DNA molecules and the effect of DNA curvature: a study by Brownian dynamics simulation. *Biophys. J.* **74**, 773-779.
- Molina-López, J. A., Govantes, F. & Santero, E. (1994). Geometry of the process of transcription activation at the  $\sigma^{54}$ -dependent *nifH* promoter of *Klebsiella pneumoniae*. *J. Biol. Chem.* **269**, 25419-25425.
- Mossing, M. C. & Record, M. T., Jr. (1986). Upstream operators enhance repression of the lac-promoter. *Science*, **233**, 889-892.
- Müller, H.-P., Sogo, J. M. & Schaffner, W. (1989). An enhancer stimulates transcription in trans when attached to the promoter via a protein bridge. *Cell*, **58**, 767-777.
- Munteanu, M. G., Vlahovicek, K., Parthasarathy, S., Simon, I. & Pongor, S. (1998). Rod models of DNA: sequence-dependent anisotropic elastic modelling of local bending phenomena. *Trends Biochem. Sci.* **23**, 341-347.
- Ninfa, A. J., Reitzer, L. J. & Magasanik, B. (1987). Initiation of transcription at the bacterial *glnAp2* promoter by purified *E. coli* components is facilitated by enhancers. *Cell*, **50**, 1039-1046.
- Pfannschmidt, C. & Langowski, J. (1998). Superhelix organization by DNA curvature as measured through site-specific labeling. *J. Mol. Biol.* **275**, 601-611.
- Porter, S. C., North, A. K. & Kustu, S. (1995). Mechanism of transcriptional activation by NTRC. In *Two-component Signal Transduction* (Hoch, J. A. & Silhavy, T. J., eds), pp. 147-158, ASM Press, Washington, DC.
- Pruss, G. J. & Drlica, K. (1989). DNA supercoiling and prokaryotic transcription. *Cell*, **56**, 521-523.
- Ptashne, M. & Gann, A. (1997). Transcriptional activation by recruitment. *Nature*, **386**, 569-577.
- Reitzer, L. J. & Magasanik, B. (1983). Isolation of the nitrogen assimilation regulator NRI, the product of the *glnG* gene of *Escherichia coli*. *Proc. Natl Acad. Sci. USA*, **80**, 5554-5558.
- Reitzer, L. J. & Magasanik, B. (1986). Transcription of *glnA* in *E. coli* is stimulated by activator bound to sites far from the promoter. *Cell*, **45**, 785-792.
- Reitzer, L. J., Movsas, B. & Magasanik, B. (1989). Activation of *glnA* transcription by nitrogen regulator I (NRI)-phosphate in *Escherichia coli*: evidence for a long-range physical interaction between NRI-phosphate and RNA polymerase. *J. Bacteriol.* **171**, 5512-5522.
- Révet, B., Brahms, S. & Brahms, G. (1995). Binding of the transcription activator NRI (NTRC) to a supercoiled DNA segment imitates association with the natural enhancer: an electron microscopic investigation. *Proc. Natl Acad. Sci. USA*, **92**, 7535-7539.
- Révet, B., von Wilcken-Bergmann, B., Bessert, H., Barker, A. & Müller-Hill, B. (1999). Four dimers of lambda repressor bound to two suitably spaced pairs of lambda operators form octamers and DNA loops over large distances. *Curr. Biol.* **9**, 151-154.
- Rice, P. A. (1997). Making DNA do a U-turn: IHF and related proteins. *Curr. Opin. Struct. Biol.* **7**, 86-93.
- Rice, P. A., Yang, S., Mizuuchi, K. & Nash, H. A. (1996). Crystal structure of an IHF-DNA complex: a protein-induced DNA U-turn. *Cell*, **87**, 1295-1306.
- Ringrose, L., Chabanis, S., Angrand, P. O., Woodroffe, C. & Stewart, A. F. (1999). Quantitative comparison of DNA looping *in vitro* and *in vivo*: chromatin increases effective DNA flexibility at short distances. *EMBO J.* **18**, 6630-6641.
- Rippe, K. (2000). Simultaneous binding of two DNA duplexes to the NtrC-enhancer complex studied by two-color fluorescence cross-correlation spectroscopy. *Biochemistry*, **39**, 2131-2139.
- Rippe, K., von Hippel, P. H. & Langowski, J. (1995). Action at a distance: DNA-looping and initiation of transcription. *Trends Biochem. Sci.* **20**, 500-506.
- Rippe, K., Guthold, M., von Hippel, P. H. & Bustamante, C. (1997). Transcriptional activation via DNA-looping: visualization of intermediates in the activation pathway of *E. coli* RNA polymerase- $\sigma^{54}$  holoenzyme by scanning force microscopy. *J. Mol. Biol.* **270**, 125-138.
- Rippe, K., Mücke, N. & Schulz, A. (1998). Association states of the transcription activator protein NtrC from *E. coli* determined by analytical ultracentrifugation. *J. Mol. Biol.* **278**, 915-933.
- Santero, E., Hoover, T. R., North, A. K., Berger, D. K., Porter, S. C. & Kustu, S. (1992). Role of integration host factor in stimulating transcription from the  $\sigma^{54}$ -dependent *nifH* promoter. *J. Mol. Biol.* **227**, 602-620.
- Satchwell, S. C., Drew, H. R. & Travers, A. A. (1986). Sequence periodicities in chicken nucleosome core DNA. *J. Mol. Biol.* **191**, 659-675.
- Schätz, T. & Langowski, J. (1997). Curvature and sequence analysis of eukaryotic promoters. *J. Biomol. Struct. Dynam.* **15**, 265-275.
- Schulz, A., Mücke, N., Langowski, J. & Rippe, K. (1998). Scanning force microscopy of *E. coli* RNA polymerase- $\sigma^{54}$  holoenzyme complexes with DNA in buffer and in air. *J. Mol. Biol.* **283**, 821-836.
- Shore, D. & Baldwin, R. L. (1983). Energetics of DNA twisting. I. Relation between twist and cyclization probability. *J. Mol. Biol.* **179**, 957-981.
- Shore, D., Langowski, J. & Baldwin, R. L. (1981). DNA flexibility studied by covalent closure of short fragments into circles. *Proc. Natl Acad. Sci. USA*, **78**, 4833-4837.
- Su, W., Porter, S., Kustu, S. & Echols, H. (1990). DNA-looping and enhancer activity: association between DNA-bound NtrC activator and RNA polymerase at the bacterial *glnA* promoter. *Proc. Natl Acad. Sci. USA*, **87**, 5504-5508.
- Trifonov, E. N. & Sussman, J. L. (1980). The pitch of chromatin DNA is reflected in its nucleotide sequence. *Proc. Natl Acad. Sci. USA*, **77**, 3816-3820.

- Trifonov, E. N. & Ulanovsky, L. E. (1988). Inherently curved DNA and its structural elements. In *Unusual DNA Structures* (Wells, R. D. & Harvey, S. C., eds), pp. 173-187, Springer Verlag, New York.
- Vologodskii, A. V., Levene, S. D., Klenin, K. V., Frank-Kamenetskii, M. D. & Cozzarelli, N. R. (1992). Conformational and thermodynamic properties of supercoiled DNA. *J. Mol. Biol.* **227**, 1224-1243.
- Wedel, A. & Kustu, S. (1995). The bacterial enhancer-binding protein NTRC is a molecular machine: ATP hydrolysis is coupled to transcriptional activation. *Genes Dev.* **9**, 2042-2052.
- Wedel, A., Weiss, D. S., Popham, D., Dröge, P. & Kustu, S. (1990). A bacterial enhancer functions to tether a transcriptional activator near a promoter. *Science*, **248**, 486-490.
- Wedemann, G., Münkkel, C., Schoppe, G. & Langowski, J. (1998). Kinetics of structural changes in superhelical DNA. *Phys. Rev. ser. E*, **58**, 3537-3546.
- Weiss, V., Claverie-Martin, F. & Magasanik, B. (1992). Phosphorylation of nitrogen regulator I of *Escherichia coli* induces strong cooperative binding to DNA essential for activation of transcription. *Proc. Natl Acad. Sci. USA*, **89**, 5088-5092.
- Whitehall, S., Austin, S. & Dixon, R. (1992). DNA supercoiling response of the  $\sigma^{54}$ -dependent *Klebsiella pneumoniae* *nifL* promoter *in vitro*. *J. Mol. Biol.* **225**, 591-607.
- Wu, H. M. & Crothers, D. M. (1984). The locus of sequence-directed and protein-induced DNA bending. *Nature*, **308**, 509-513.

*Edited by K. Yamamoto*

*(Received 17 February 2000; received in revised form 22 May 2000; accepted 29 May 2000)*